JVSTA
JOURNAL OF VACUUM SCIENCE AND TECHNOLOGY A

Effects of the plasmawall sheath on transport

J. Mandrekas, C. E. Singer, and D. N. Ruzic

Citation: J. Vac. Sci. Technol. A **5**, 2315 (1987); doi: 10.1116/1.574443
View online: http://dx.doi.org/10.1116/1.574443
View Table of Contents: http://avspublications.org/resource/1/JVTAD6/v5/i4
Published by the AVS: Science & Technology of Materials, Interfaces, and Processing

Effects of the plasma-wall sheath on transport

J. Mandrekas, C. E. Singer, and D. N. Ruzic
University of Illinois, Urbana, Illinois 61801

(Received 19 September 1986; accepted 24 November 1986)

The 1½-dimensional plasma transport code BALDUR, along with the neutral transport code DEGAS are used to study the effects of secondary and photoelectron emission from the wall and limiters of a tokamak on the plasma transport. Since different electron emission mechanisms appear to be dominant in different parts of the scrapeoff, the two-region scrapeoff model included in BALDUR is particularly useful. The effect that secondary and photoelectron emission have on recycling through the reduction of the sheath potential is taken into account in DEGAS by prescribing appropriate values of the sheath potential on each recycling surface, according to the dominant electron emission mechanism present. Results indicate that when photoelectron emission from the first wall increases, the ion and electron temperatures increase in the scrapeoff, while they remain unaffected near the center. When the secondary electron coefficient of the limiters is increased, the ion and electron temperatures drop in the scrapeoff while they increase near the center. In both cases the neutral density decreases slightly throughout the device.

I. INTRODUCTION

When a solid surface is in contact with a plasma, an electrostatic sheath is formed in order to balance the electron and ion fluxes to the surface. In a tokamak such sheaths are attached to the limiters or divertor plates and the first wall. The presence of the sheath can have a significant influence on the plasma transport in the scrapeoff layer, and consequently on the plasma properties in the device: (a) It affects the recycling since ions are accelerated by the sheath potential before they hit the surface, which influences the energy and number that are returned to the plasma as neutrals, and (b) the energy and particle removal rates at the scrapeoff along the field lines are controlled by the sheath potential.

The magnitude of the sheath potential is given by[1]

$$\frac{eV_f}{T_e} = 0.5 \ln\left[\left(2\pi\frac{M_e}{M_i}\right)\left(1+\frac{T_i}{T_e}\right)(1-\Gamma)^{-2}\right] \tag{1}$$

and the electron energy removal rate from the plasma along the field lines is $P_e = 2T_e n_e u_s \gamma_e$, where u_s is the sound speed, $u_s = [(T_e + T_i)/m_i]^{1/2}$ (Bohm criterion), and γ_e is the sheath energy transmission factor[1]

$$\gamma_e = \frac{1}{1-\Gamma} - \frac{1}{2}\frac{eV_f}{T_e}. \tag{2}$$

In Eqs. (1) and (2), V_f is the sheath potential, T_i and T_e the ion and electron temperatures, respectively, and Γ is the overall secondary electron coefficient which includes electron impact secondary electron emission and photoelectron emission. Γ is given by

$$\Gamma = \frac{\delta_e + j}{1+j}, \tag{3}$$

where δ_e is the electron impact secondary electron emission coefficient and $j = J/n_e u_s$ with J being the photoelectron flux.

The above relations show that by increasing secondary electron emission the sheath potential V_f is reduced while the sheath energy transmission factor for the electrons γ_e is increased.

Formulas (1) and (2) neglect the contribution of the presheath voltage drop which is of the order of $(1/2)kT_e/e$. Also in Eq. (2) it has been assumed that the thermal energy of secondary electrons is negligible. This is a good approximation for secondary electrons arising from electron impact, but not for photoelectrons, since sometimes they are born with the energy of several electron volts. For cases with appreciable photoelectron contributions Eq. (2) should be modified to

$$\gamma_e = \frac{1}{1-\Gamma} - \frac{1}{2}\frac{eV_f}{T_e} - \frac{1}{2}\frac{\Gamma-\delta_e}{1-\Gamma}\frac{E_0}{T_e}, \tag{4}$$

where E_0 is the average energy of the emitted photoelectrons.

Near the limiters, T_e is relatively high and j is small, since the flux $n_e u_s$ is much higher than the photoelectron flux. So from Eq. (3), $\Gamma \simeq \delta_e$, i.e., the dominant emission mechanism in this region is electron impact secondary electron emission. On the other hand, near the wall where the electron temperature T_e is small, δ_e is negligible, but j can be near one (see Sec. III). So photoelectron emission can be the dominant mechanism in this part of the scrapeoff.

In this work we tried to study the relative effect of secondary electron emission from the limiters and photoelectron emission from the wall on the plasma transport. Studies of the effect of secondary electron emission on the plasma parameters in the scrapeoff have been done before,[2,3] but this appears to be the first time that different emission mechanisms have been taken into a account in a self-consistent way.

II. MODEL

A. Plasma model

Version BALDNO9M of the 1½-dimensional transport code BALDUR[4] is used. It solves the flux-surface-averaged transport equations[5]

 0734-2101/87/042315-04$01.00

$$\frac{1}{V'}\frac{\partial(V'n_a)}{\partial t}+\frac{1}{V'}\frac{\partial(V'\Gamma_a)}{\partial\rho}=S_a\,, \tag{5}$$

$$\frac{1}{(V')^{5/3}}\frac{\partial\left[(V')^{5/3}E_j\right]}{\partial t}+\frac{1}{V'}\times\frac{\partial\{V'[-n_j\chi_j(\partial T_j/\partial\rho)+v_jT_j\Gamma_j]\}}{\partial\rho}=S_j \tag{6}$$

along with an equation for the poloidal magnetic flux ψ and the radial pressure balance. Here V is the volume within a flux surface labeled by ρ, $'$ denotes $\partial/\partial\rho$, and ρ is taken to be the half-width of a magnetic flux surface on the toroidal midplane. The following quantities are averaged over a magnetic flux surface: the partial and total ion densities n_a and n_i, the ion particle fluxes and sources Γ_a and S_a, the ion and electron energy densities E_i and E_e, the ion and electron thermal diffusivities χ_i and χ_e, the ion and electron temperatures T_i and T_e, and the ion and electron energy sources S_i and S_e.[3] Semiempirical transport coefficients were used, based on the modified neoalcator model of Singer *et al.*,[6] with $\alpha_e=1.5$ and $\chi_i=\chi_e/2$, and particle diffusion coefficient $D=\chi_e/5$. χ_e is limited to less than $10\,\chi_{\text{Bohm}}$, where $\chi_{\text{Bohm}}=1.5cT_e/(16eB)$, using the transformation,

$$\chi_e\rightarrow\frac{\chi_e\chi_B}{\chi_e+\chi_B}\,. \tag{7}$$

Of all the different contributions to the source terms S_a, S_i, and S_e the scrapeoff losses are the most important to our work. They represent losses due to flow along the field lines to the limiter or to the material wall and are written as

$$S_a^s=-\frac{n_a}{\tau_\parallel}\,, \tag{8}$$

$$S_e^s=-\frac{2\gamma_eE_e}{\tau_\parallel}\,, \tag{9}$$

$$S_i^s=-\frac{2E_i}{\tau_\parallel}\,, \tag{10}$$

where γ_e is the sheath transmission factor defined in the introduction and $\tau_\parallel=L/(Mu_s)$, where L is the characteristic length of the scrapeoff, and M is the parallel Mach number determined by a "two-chamber" model[7] which integrates the fluid equations along the field lines between a sonic flow at the material boundary and a subsonic flow in the main scrapeoff. For the simulations below, M was around 0.5.

The scrapeoff layer itself consists of two regions (see Fig. 1): the first contains the field lines that intercept the limiter surface. Its characteristic length is taken to be the connection length πRq where R is the major radius and q is the safety factor, since a field line must travel around the torus q times from the limiter before encountering it again. The second scrapeoff region consists of those magnetic field lines which, due to the shifting of the magnetic surfaces, intercept the material wall first before they intercept the limiter. The theoretical length of this scrapeoff should be πr, but due to the presence of various constructions near the wall, it can practically assume any value between πr and πRq. For this simulation, it is taken to be 500 cm.

The two-region scrapeoff model allows us to include in a self-consistent manner, the effect that different emission mechanisms have on plasma energy transport by prescribing different energy transmission factors in the two regions.

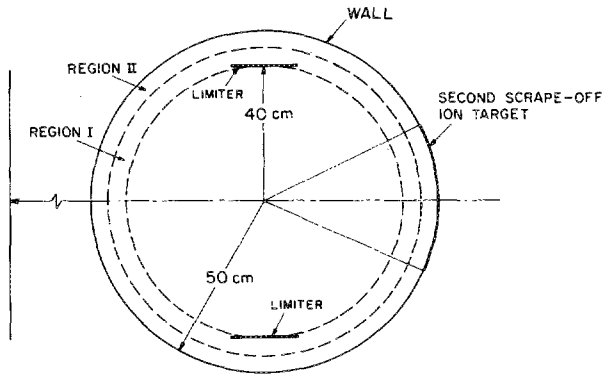

FIG. 1. Poloidal cross section of PLT, showing the boundaries of the first and second scrapeoff regions I and II, the positions of the two carbon limiters, and the part of the wall which acted as a limiter.

B. Neutral models

BALDUR contains the one-dimensional Monte Carlo code AURORA[8] to calculate the neutral transport and the various source terms needed in the plasma calculations. A fraction of the lost ions (both in the parallel and perpendicular directions) determined by the recycling coefficient is returned to the plasma as neutral atoms. To simulate the effect of the sheath on the recycling, the energy of these incoming neutrals is taken to be equal to eV_f, where V_f is the sheath potential as given by Eq. (1) using $\langle T_e\rangle$, the average electron temperature in the scrapeoff, as T_e.

AURORA though, being one dimensional, cannot treat the geometry of the device accurately and it cannot distinguish between neutrals recycled from the limiter and neutrals recycled from the wall. To include geometric effects and to study the effect of varying the secondary and photoelectron coefficients of the wall and limiter separately, as well as to include molecular recycling, the three-dimensional Monte Carlo code DEGAS[9] was linked with BALDUR. The effect that electron emission has on recycling through the reduction of the sheath potential, is taken into account by taking the energy of the neutrals launched in DEGAS to be T_i+eV_f, where T_i is sampled from a Maxwellian at the local ion temperature and V_f is the sheath potential as given by Eq. (1). To simulate recycling from the first wall due to the second scrapeoff, a portion of the wall is treated as a neutralizing plate for recycling purposes: Plasma particle losses due to parallel flow [cf. Eq. (7)], from the second scrapeoff are recycled from that part of the wall designated as second scrapeoff ion target in Fig. 1.

III. RESULTS

A well-documented PLT discharge with $\bar{n}_e=1\times10^{13}$ cm^{-3} served as the basis of our simulations. In Fig. 2, the points and error bars for T_e and n_e are from TVTS measurements, extended by general probe results.[10] In Fig. 3, T_i and

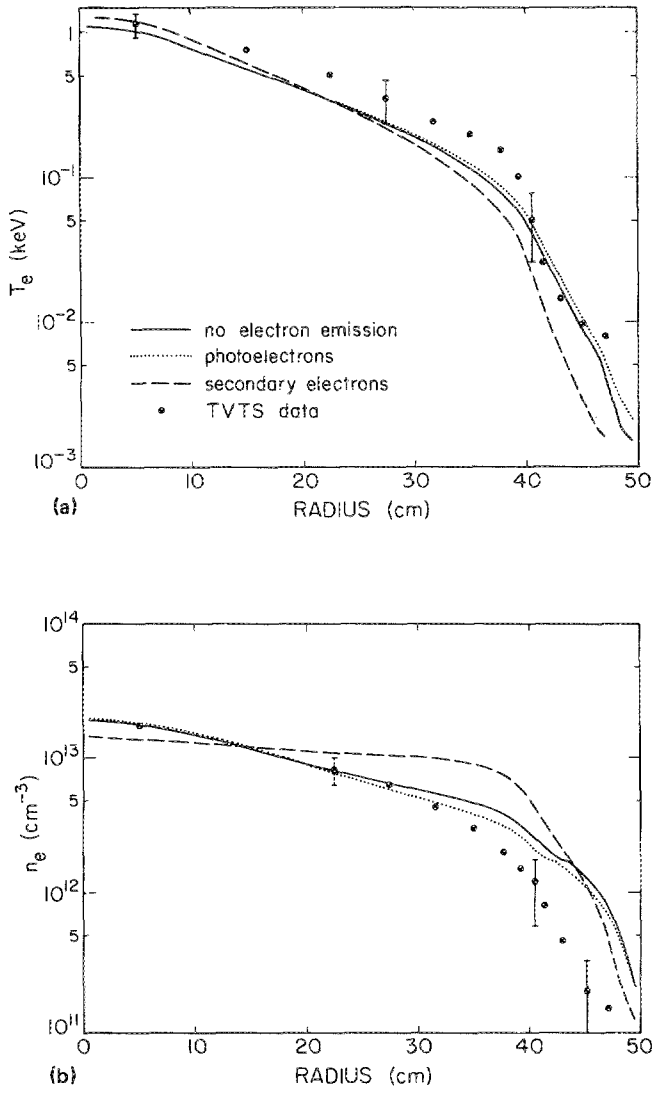

FIG. 2. Calculated profiles for the cases of — no secondary emission, ··· photoelectron emission from the wall, and - - - secondary electron emission from the limiters. The points and error bars are from TVTS measurements: (a) electron temperature; (b) electron density.

n_0 points are from simulations based on neutral efflux measurements.[10] Here, it must be emphasized that we did not try to match the experimental results. Rather, the experimental results were used to help us adjust a number of parameters in the code such as the relative thickness of the two scrapeoff layers, the Bohm-diffusion limit, and the collisional ion–electron energy interchange terms, and to also ensure that the predictions of the model were somewhat realistic.

Sawtooth oscillations were included with a period of 10 ms, and Z_{eff} was taken to be 1.5. In order to approach the high ion temperatures reported in this discharge, the collisional ion–electron energy interchange had to be significantly increased by a factor of 6.5; while anomalous interchange is predicted theoretically,[11] it is not clear that the present theory would account for such a large factor.

In DEGAS an approximation of the true geometry of the two carbon limiters was used[12] (cf. Fig. 1). The ion flux in the first scrapeoff, as calculated by BALDUR, was evenly divided between the two limiters, while the ion flux in the second scrapeoff was directed to a portion of the wall of the device. The thickness of the outer scrapeoff was adjusted in such a way that the ratio of the ion flux onto the limiters versus the ion flux onto the wall was approximately 5.6, a value that is close to the observed ratio of 6.3.[10] To minimize computer time, each simulation began with AURORA as the neutral model and switched to DEGAS at approximately 450 ms.

Three different cases were studied: In the first, no secondary electron emission of any kind was assumed. The values of the sheath potential and the energy transmission coefficient were taken from Eqs. (1) and (2) assuming $\Gamma = 0$. In Figs. 2 and 3 this case is represented by the solid line. The transport

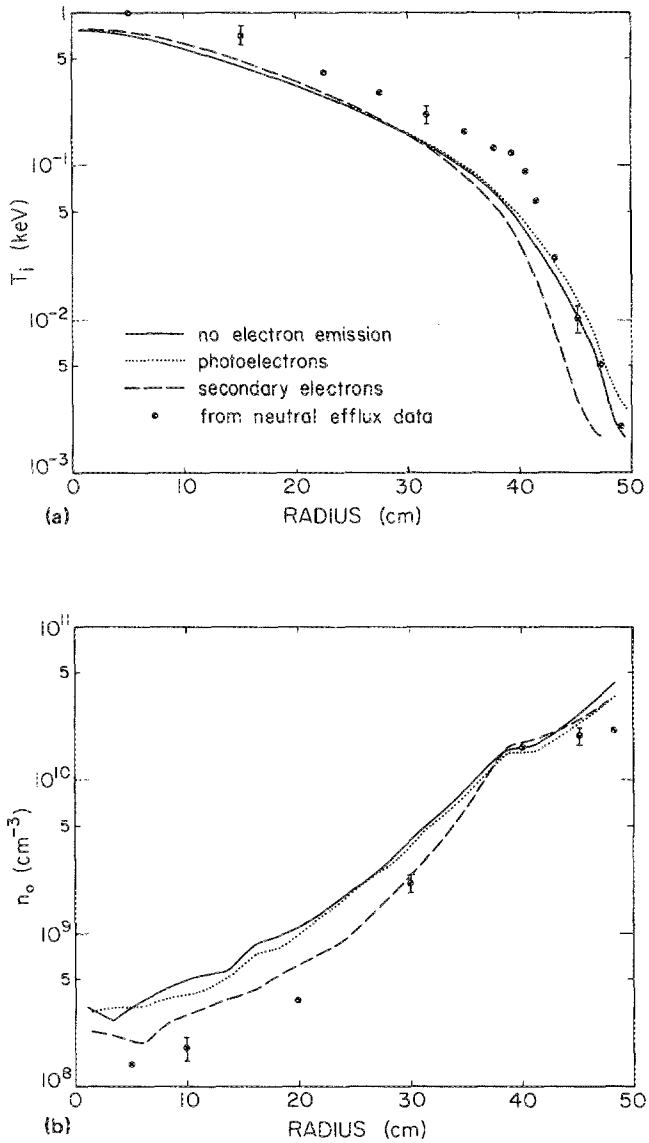

FIG. 3. Calculated profiles for the cases of — no secondary emission, ··· photoelectron emission from the first wall, and - - - secondary electron emission from the limiters. The points and error bars are from simulations based on neutral efflux measurements: (a) ion temperature; (b) neutral density.

model gives reasonable agreement with most of the reported profiles, although the discrepancy with the electron density in the scrapeoff is significant. Although our goal was not to match the experimental results, inclusion of processes like the impurity pinch could help reduce the density near the edge.

In the second case, an attempt was made to study the effect of enhanced electron emission from the wall. Since the electron temperature in the outer scrapeoff is rather small (2–5 eV) secondary emission due to electron impact is not expected to be significant. On the other hand, photon fluxes can be as high as 10^{16} photons/s cm^2 from O V (630 Å, 760 Å), and C III (977 Å).[13] In specially prepared surfaces the photoelectron coefficient can be as high as 0.2 for this energy range (12–20 eV),[14] leading to a total secondary coefficient Γ, equal to 0.64. This results in a drop of the sheath potential of the first wall to $1.7T_e$, while the potential of the two limiters is kept at $2.83T_e$, corresponding to $\Gamma = 0$. The energy transmission coefficient in the second scrapeoff is calculated from Eq. (4) assuming a ratio of E_0 vs T_e of 3. The results of this simulation are represented with the dotted lines in Figs. 2 and 3. As can be seen, the plasma at the center is not affected while in the scrapeoff the electron and ion temperatures increase and the electron and neutral densities drop slightly.

Finally, in the third case, the secondary electron coefficient Γ in the first scrapeoff was assumed to be equal to 0.8. This value is high but is obtainable from carbon at 100 eV for grazing incidence.[15] Since near the limiters electron temperature can be high, electron impact is the dominant emission mechanism and Γ can be taken to be equal to δ_e. Then, from Eqs. (1) and (2), the sheath potential of the limiters was $1.23T_e$ and the energy transmission factor γ_e was 5.6. The sheath potential and energy transmission factor of the first wall were taken to correspond to the $\Gamma = 0$ case. The results are shown in Figs. 2 and 3 (dashed line). It can be seen that in this case, the electron and ion temperatures drop in the scrapeoff while they increase at the center. The neutral density drops throughout the device, and the electron density profile is flattened before it drops at the scrapeoff.

IV. DISCUSSION AND CONCLUSIONS

The goal of this work was to study the effect that electron emission in the scrapeoff can have on the plasma properties. Since different electron emission mechanisms appear to be dominant in different parts of the scrapeoff, we studied the case of secondary electron emission from the limiters and photoelectron emission from the wall. Secondary electron emission increases the electron energy transmission factor γ_e, hence the electron energy loss along the field lines in the scrapeoff, while photoelectron emission can help to decrease the losses by adding energy into the plasma. Using the two-region scrapeoff model contained in BALDUR, we were able to take these effects into account.

Both secondary and photoelectron emission lower the sheath potential of the surface and this affects the recycling. This effect was also taken into account in DEGAS by prescribing different potentials on the limiters and the wall depending on the emission mechanisms assumed.

It was found that secondary and photoelectron emission can both have an impact on the plasma properties in a tokamak: Increased secondary emission from the limiters results in a reduction of the electron and ion temperatures in the scrapeoff and a rise near the center. Increased photoelectron emission from the wall causes the electron and ion temperatures in the scrapeoff to increase, while they remain unaffected near the center. The reduced sheath potential in both cases causes the neutrals to be launched with lower energies resulting in a neutral density drop throughout the device. This effect seems to be more significant in the case of secondary emission from the limiters since most of the recycling takes place there.

The design of future structures that lie in the scrapeoff regions may be able to utilize these effects to influence the behavior of the plasma.

ACKNOWLEDGMENTS

The authors would like to thank D. Heifetz of Princeton Plasma Physics Laboratory, Princeton University (PPPL) for his help in the linking of DEGAS and BALDUR; G. Bateman of PPPL for the version of the BALDUR code used as a starting point for these studies; C. Daughney for the TVTS measurements; and G. Hrbek of the University of Illinois for initial discussions. This work was supported in part by the NSF and by the U.S. DOE Contract No. DE-AC02-76-CHO-3073.

[1]P. C. Stangeby, in *Physics of Plasma-Wall Interactions in Controlled Fusion*, edited by D. E. Post and R. Behrisch (Plenum, New York, 1986).
[2]G. Fuchs and A. Nicolai, Nucl. Fusion **20**, 1247 (1980).
[3]P. J. Harbour and M. F. Harrison, J. Nucl. Mater. **76/77**, 513 (1978).
[4]C. E. Singer, D. E. Post, D. R. Mikkelsen, M. H. Redi, A. McKenney, A. Silverman, F. G. P. Seidel, P. H. Rutherford, R. J. Hawryluk, W. D. Langer, L. Foote, D. B. Heifetz, W. A. Houlberg, M. H. Hughes, R. V. Jensen, G. Lister, and J. Ogden, Princeton University Plasma Physics Laboratory Report No. PPPL-2073, 1986.
[5]C. E. Singer, G. Bateman, and L. P. Ku, Princeton University Plasma Physics Laboratory Report No. PPPL-2414, 1987.
[6]C. E. Singer, L. P. Ku, G. Bateman, F. Seidl, and M. Sugihara, in *Proceedings of the Eleventh Symposium on Fusion Engineering* (IEEE, Austin, 1985), Vol. 1, p. 41.
[7]W. D. Langer and C. E. Singer, IEEE Trans. Plasma Sci. **13**, 163 (1985).
[8]M. H. Hughes and D. E. Post, J. Comput. Phys. **28**, 43 (1978).
[9]D. Heifetz, D. Post, M. Petravic, and G. Bateman, J. Comput. Phys. **46**, 309 (1982).
[10]D. N. Ruzic, D. Heifetz, and S. A. Cohen, J. Nucl. Mater. (in press).
[11]R. R. Dominguez and R. E. Waltz, GA Technologies Report No. GA-A18184, 1986.
[12]S. A. Cohen, R. Budny, G. M. McCracken, and M. Ulrickson, Nucl. Fusion **21**, 233 (1981).
[13]B. C. Stratton, A. T. Ramsey, S. T. Boody, C. E. Bush, R. J. Fonck, R. J. Groebner, R. A. Hulse, R. K. Richards, and J. Schivell, Nucl. Fusion (accepted).
[14]A. H. Sommer, *Photoemissive Materials* (Wiley, New York, 1968), p. 34, and references therein.
[15]D. Ruzic, R. Moore, D. Manos, and S. Cohen, J. Vac. Sci. Technol. **20**, 1313 (1982).